Kinetics of radiation-induced segregation in Ni—12.7 at. % Si

R. S. Averback, L. E. Rehn, W. Wagner, H. Wiedersich, and P. R. Okamoto
Materials Science Division, Argonne National Laboratory, Argonne, Illinois 60439
(Received 14 March 1983)

The kinetics of radiation-induced segregation in Ni—12.7 at. % Si alloys was investigated using *in situ*, simultaneous Rutherford-backscattering spectrometry. It was observed that a precipitate layer of γ'—Ni_3Si grew at the specimen surface during 2.0-MeV He and 2.75-MeV Li irradiations. The thickness of the γ' layer was measured as a function of dose, dose rate, and temperature. For all of the irradiation conditions the γ' layer thickness grew proportionately to the square root of dose. The proportionality constant, or growth-rate constant, was dependent on temperature and dose rate. Below ~ 570 °C the growth-rate constant displayed Arrhenius behavior with an apparent activation enthalpy of 0.30 ± 0.04 eV, and it depended approximately on the $-\frac{1}{4}$th power of the dose rate. Above 590 °C the growth-rate constant also displayed Arrhenius behavior but with an apparent activation enthalpy of -0.75 ± 0.15 eV; moreover, it was independent of dose rate in this temperature regime. A simple model for radiation-induced segregation is described which relates the segregation results to high-temperature point-defect properties in alloys. It shows that the apparent activation enthalpy of the growth-rate constant at low temperatures is equal to $\frac{1}{4}$ the enthalpy of vacancy migration, and that at high temperatures it is equal to $-\frac{1}{2}$ the enthalpy of vacancy formation. The model also correctly predicts the observed dose-rate dependences of the growth-rate constant in the two temperature regimes.

I. INTRODUCTION

Irradiation of metals with energetic particles at elevated temperatures induces point-defect fluxes. In many alloys these fluxes couple preferentially to solute atoms and thus transport them disproportionately to their relative concentrations in the bulk. Consequently changes in the local composition and phase of an alloy can occur in regions which experience a net flux of defects. This effect, radiation-induced segregation (RIS) was first observed in stainless steel,[1] and has since been reported to occur in many other alloy systems. RIS is now recognized as a common phenomenon in irradiated alloys. It is of considerable interest because of its importance to the phase stability of materials in reactor environments, and to the new technology of using ion beams to modify materials.

Previous studies of RIS have concentrated on establishing the conditions under which RIS occurs, and characterizing the microstructural changes which are induced by RIS.[2–4] These studies have examined the influence of temperature, alloy concentration, and irradiation conditions on the occurrence of RIS. They have also investigated which new phases appear under irradiation, and where the new phases nucleate and grow. Such studies are necessary because equilibrium phase diagrams cannot be used reliably to predict stable phases in a nonequilibrium radiation environment. However, to critically assess current theories of RIS, and to relate the observed segregation effects to fundamental properties of point defects, quantitative kinetic information on RIS is required. In this paper we report on the kinetics of RIS in a Ni—12.7 at. % Si alloy.

It has been observed in previous studies of RIS in Ni-Si alloys that γ', an ordered Ni_3Si compound, precipitates as a layer on irradiated surfaces of Ni-Si alloys.[5] In this study we have measured the growth kinetics of this γ' layer, i.e., the dose, dose-rate, and temperature dependences. A novel, *in situ* procedure using simultaneous Rutherford-backscattering spectrometry was employed to accurately measure the segregation during irradiation. In addition a theoretical model is presented to describe the growth kinetics of the γ' layer. It will be shown that the RIS kinetics in Ni-Si can be related to point-defect properties in alloys using a rather simple segregation model.

II. EXPERIMENTAL

High-resolution Rutherford-backscattering spectrometry (RBS) was employed to determine the flux of Si to the surface of a Ni—12.7 at. % Si alloy during He and Li irradiations. The solubility of Si in Ni is ~ 10 at. % at 600 °C. During irradiation, however, alloys containing as little as 1 at. % Si become two phase due to RIS.[6] The 12.7 at. % Ni-Si alloy was selected because its microstructural development during irradiation had been well characterized in previous studies,[5] and also because it was known to acquire thick precipitate coatings whose thicknesses [5—50 nm (Ref. 7)] could be accurately measured. The backscattering technique is particularly useful for light-ion irradiations since the irradiation beam itself can be employed for simultaneous RBS analysis. This procedure has several advantages in comparison with standard post-irradiation specimen analysis. The major advantages are as follows: It eliminates the possibility for compositional changes to occur after the completion of an irradiation but before or during the analysis, as for exam-

ple, by thermal diffusion during the cooling of a specimen irradiated at high temperature, or during sputter profiling. For measurements of the dose dependence this procedure eliminates errors associated with variations in specimen microstructure or purity since the same specimen is employed for the entire experiment. The analysis is nondestructive and therefore preserves the specimen for subsequent analysis by other techniques. In addition simultaneous RBS provides an accurate measurement of the ion dose (and dose rate) since the backscattered yield is directly proportional to the ion current impinging on the specimen. Lastly, the experimental technique can be employed simply and quickly and thus it is suitable for survey studies of many different alloy systems, as well as for detailed investigations of a particular system.[8]

A. Rutherford-backscattering spectrometry

Figure 1(a) illustrates a computer-generated backscattering spectrum for a Ni—12.7 at.% Si alloy with and without a 35-nm-thick γ'-Ni_3Si surface film. The backscattered yield, $H_{Ni}(E)$ results from incoming particles backscattering with energy E from Ni atoms. The precipitous drop in yield at the high-energy end of the spectrum is designated the Ni "leading edge." The leading edge of the lighter Si atoms is superposed at a lower energy onto the yield from Ni at some depth. The composition of the unirradiated alloy can be determined from the relative magnitudes of H_{Ni} and H_{Si}. The ratio H_{Si}/H_{Ni} is approximately equal to the product of the ratio of the scattering cross sections for Si and Ni and their relative concentrations. Thus $H_{Si}/H_{Ni} \approx 0.04$ for Ni—12.7 at.% Si. The increase of the Si concentration in the surface region during irradiation results in an increase in $H_{Si}, \Delta H_{Si}$, and a decrease in $H_{Ni}, \Delta H_{Ni}$, which occur at and behind the Si and Ni leading edges, respectively. The ratio $\Delta H_{Ni}/\Delta H_{Si} \approx -3$ for the formation of a Ni_3Si surface layer on a Ni—12.7 at.% Si alloy, and so the absolute change in the Ni yield is more sensitive to concentration changes than is the change in the Si yield. On the other hand, the relative change in the Si yield is greater, $\Delta H_{Si}/H_{Si} \approx 1.0$, whereas $\Delta H_{Ni}/H_{Ni} \sim 0.15$. Moreover ΔH_{Si} is, to a good approximation, sensitive only to changes in the Si concentration, whereas ΔH_{Ni} depends on changes in the concentration of any atomic species at the surface. It is therefore prudent to analyze both the Ni and Si yields.

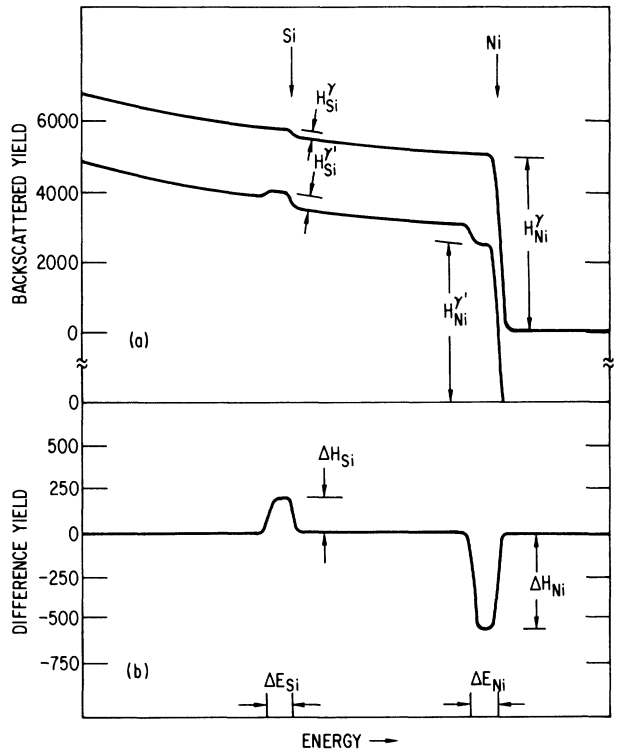

FIG. 1. (a) Computer generated RBS spectra for a uniform Ni—12.7 at.% Si alloy and for the same alloy containing a 35-nm-thick γ'-Ni_3Si layer at the surface. (b) Difference spectra for the two RBS spectra in (a).

The energy resolution of the RBS system ΔE_0 was ~ 20 keV, which for the scattering geometry employed here corresponds to a depth resolution Δx_0 of ~ 6 nm.[9] This value of Δx_0 does not represent the thinnest film that can be detected, nor the smallest change in a growing film that can be resolved. Rather, it means that atoms located at the depth x will contribute to the backscattered yield in a range of energies corresponding to $\sim \Delta x_0$. For example, if a 3-nm γ' layer were on the surface of the bulk alloy, ΔH_{Ni} would be affected at energies corresponding to a depth up to ~ 9 nm. The reduction of the yield ΔH_{Ni} for this layer would be energy dependent and everywhere less than the value of ΔH_{Ni} shown in Fig. 1(a) which represents a thick γ' layer. The integral of $\Delta H_{Ni}(E)$ over the affected region, however, is linearly proportional to the γ' thickness and is independent of resolution. Therefore, the amount of Si segregation to the surface can be determined most accurately by first calculating the difference between the RBS spectra for the irradiated and the unirradiated specimens, and then determining the area in this difference spectrum; this area is shown for the spectra of Fig. 1(a) in the difference spectrum in Fig. 1(b).

Simultaneous RBS analysis and defect production requires that the ion dose necessary to acquire a statistically meaningful RBS spectrum be significantly smaller than that necessary to cause appreciable segregation. For our experimental conditions, a 2.0-MeV He beam ~ 0.8 mm^2 in area backscattered at 135° into a detector subtending a solid angle of $\sim 2.5 \times 10^{-4}$ sr, the integral count rate was 3×10^4/nm per displacement per atom (dpa). This means that for a dose which would produce 1 dpa, the atoms within 1 nm of the surface would scatter 3×10^4 He atoms into the detector. A spectrum with $\lesssim 1$ nm statistical uncertainty in film thickness could therefore be acquired every ~ 0.1 dpa. A major disadvantage of using He irradiation to study segregation, however, is that blistering occurs at ~ 1 dpa so that segregation at high dpa levels could not be studied. Prior to the catastrophic blistering, the implanted He had no apparent effect on RIS. The projected range of 2.0-MeV He is $\sim 2\mu$m (Ref. 10), whereas the thickest γ' films were only ~ 40 nm. In an attempt to reduce the blistering problem Li irradiation was tried. For this case doses of 5 dpa could be attained before significant surface damage occurred.

B. Experimental procedure

A Ni—12.7 at. % Si alloy was prepared by arc melting, with subsequent homogenization by induction-levitation heating. The bulk alloy was rolled into 0.75-mm-thick strips, which were solution annealed at 970 °C for six hours in argon-filled capsules and then quenched in water. The strips were mechanically polished, and then electropolished to obtain a flat smooth surface suitable for high-resolution RBS. The specimens were clamped to the heating stage of a single-axis goniometer which consisted of a thick stainless-steel tube enclosing a 400-W quartz lightbulb heating source. The axis of rotation was in the plane of the specimen surface.

The specimen temperature was determined by an infrared pyrometer which was focused onto an ~2-mm-diam spot concentric with the beam spot, and by a thermocouple which was attached directly to the specimen. The accuracy of the temperature measurement was ~10 °C; relative temperatures were determined within ~5 °C. A temperature gradient of ~6 °C cm^{-1} along the length of the specimen caused by beam heating was typical during the 2.0-MeV He irradiation as 1.6 W of beam power was required to achieve a displacement rate of $\sim 4\times10^{-4}$ dpa s^{-1}. The ion-beam dosimetry was simple and accurate for these light-ion irradiations. The beam current through a 1.0-mm-diam aperture was measured with a Faraday cup and related to the backscattered yield from the specimen. The backscattered yield was then monitored and integrated during the irradiation. A beam profile monitor was employed to check the homogeneity of the partially defocused beam. The conversion from ion-current density to dpa was performed using the computer code PINTO.[11] It was assumed for the calculation that the specimen was pure Ni and that the average displacement energy to produce a Frenkel pair in Ni is 33 eV.[12]

III. EXPERIMENTAL RESULTS

RBS spectra acquired during 2.0-MeV He irradiation at 530 °C and 556 °C are shown in Figs. 2(a) and 3(a). The time period shown above each spectrum indicates the interval during the irradiation in which the spectrum was collected. Thus each spectrum reflects the average specimen composition during the collection period as a function of depth below the surface. In both series of spectra, successive reductions in the integral Ni yield at and below the Ni leading edge are apparent; they show that the Ni concentration in the surface region decreases during irradiation. Complementary behavior is observed at and behind the Si edge where the integral Si yield increases with dose. In those spectra where a well-developed surface film can be identified, the Si concentration in the film is ~24 at. %. This agrees with previous TEM studies of irradiated Ni—12.7 at. % Si which have shown that γ'-Ni_3Si precipitates at the irradiated surface. The thickness of the γ' layers during irradiation could have been determined using the energies of the backscattered particles corresponding to the specimen surface and the back edge of the γ' layer as indicated in Fig. 1. However, a more accurate determination of the film growth rate was possible, as noted above, by analyzing the differences between the successive RBS spectra and the initial spectrum. For this purpose the spectra were normalized to correct for different acquisition times and fluctuations in the beam intensity. The normalization procedure consisted of equalizing the RBS yields in a region where no RIS is evident. The yield in the region directly in front of the Si edge was usually employed for normalization. The initial spectrum

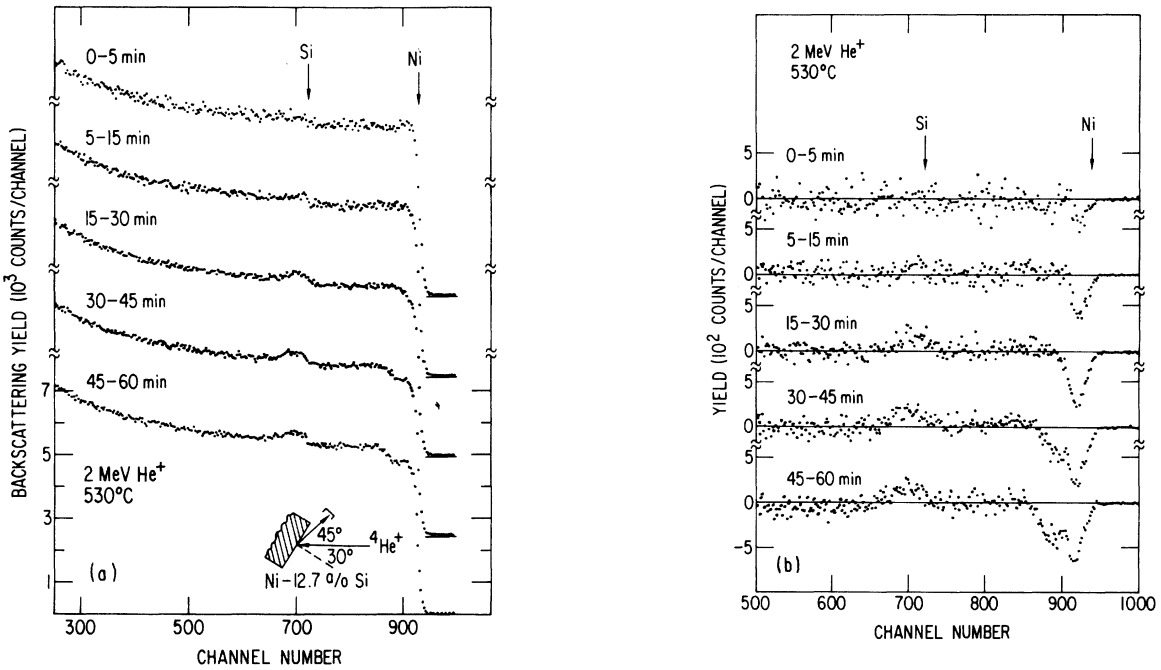

FIG. 2. (a) Series of RBS spectra collected during a 2-MeV He irradiation at 530 °C. The time intervals indicate the collection periods. (b) Difference spectra for the RBS spectra in (a).

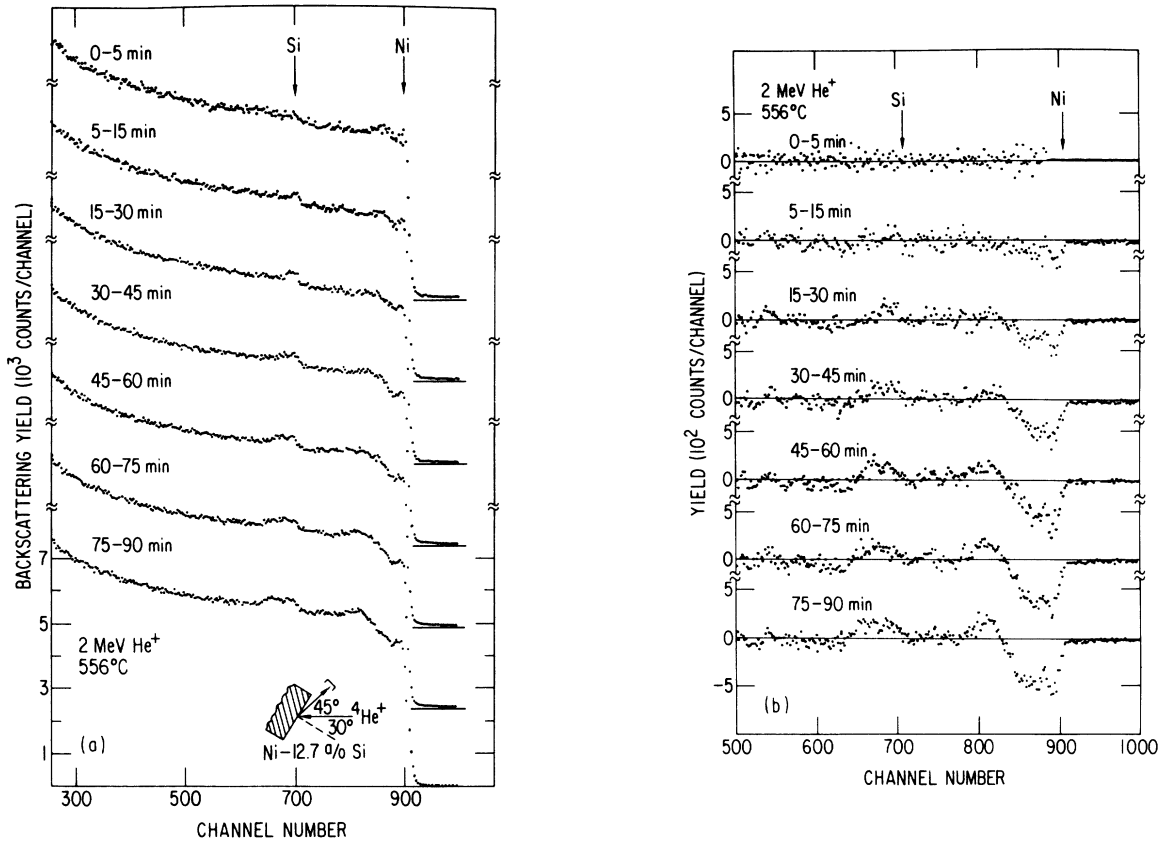

FIG. 3. (a) Series of RBS spectra collected during a 2-MeV He irradiation at 556 °C. The time intervals indicate the collection periods. (b) Difference spectra for the RBS spectra in (a).

of each series, which was collected for the shortest time interval, was smoothed by averaging counts in adjacent channels. This procedure avoids unnecessary scatter in the difference spectra. However, since it is the integral yield in the difference spectrum which determines the γ' thickness, smoothing the initial curve has no effect on the results.

In Figs. 2(b) and 3(b), difference spectra obtained from the RBS spectra in Figs. 2(a) and 3(a) are shown. Each difference spectrum represents the difference between an RBS spectrum and the appropriate, smoothed (0—5)-min spectrum. All spectra were normalized to 3500 counts per channel in front of the Si edge. The two (0—5)-min difference spectra show scatter present in the unsmoothed (0—5)-min RBS spectra. The negative yield ΔH_{Ni} which occurs behind the Ni leading edge is due to Ni depletion near the surface. Correspondingly, the positive yield behind the Si edge arises from Si enrichment near the surface. In several cases a subsurface Si depleted (Ni enriched) layer contiguous with the γ' surface layer is observed. This is revealed by both a positive ΔH_{Ni} and a negative ΔH_{Si} in the subsurface region. This Si depleted layer is clearly evident in the series of spectra collected during irradiation at 556 °C [see Fig. 3(b)].

For the standardized normalization of 3500 counts per channel in front of the Si edge, the γ' phase, with nominal composition of 23.5 at. % Si, yields calculated values of $\Delta H_{\mathrm{Ni}} = -440$ counts per channel and $\Delta H_{\mathrm{Si}} \sim 160$ counts per channel behind the Ni and Si edges, respectively. These values are in agreement with the measured yields for most of the surface layer. In some cases, and particularly noticeable for irradiations near 530 °C, the value of ΔH_{Ni} at the front of the γ' layer decreases below -440 counts per channel. This further reduction in Ni yield is consistent with the formation of the compound Ni_5Si_2 which was recently reported to form on top of the Ni_3Si layer.[13] The calculated value of ΔH_{Ni} for Ni_5Si_2 containing 28.6 at. % Si is -660 counts per channel, which is in good agreement with the values observed very close to the surface in Fig. 2(b).

Integral yields determined from difference spectra from two typical irradiations are shown in Fig. 4, plotted as a function of the square root of dose. The closed symbols represent the Ni yields, and the open symbols, the Si yields. Solid lines were drawn through the Ni data. Using these lines for the Ni yields, relative values for the Si yields were calculated as a function of dose; these yields are represented by the dashed lines. The agreement between the Ni yield and the Si yield is quite good. There does appear to be, however, a small systematic error between the Ni and Si yields for the irradiation at 502 °C. This error could arise if, for example, the surface became contaminated during irradiation. The Ni yields are more sensitive to such effects as the relative change in Ni composition when γ' is formed, is only 13% (from 87.5 to 76.5 at. %), whereas the change in the Si composition is $\sim 85\%$

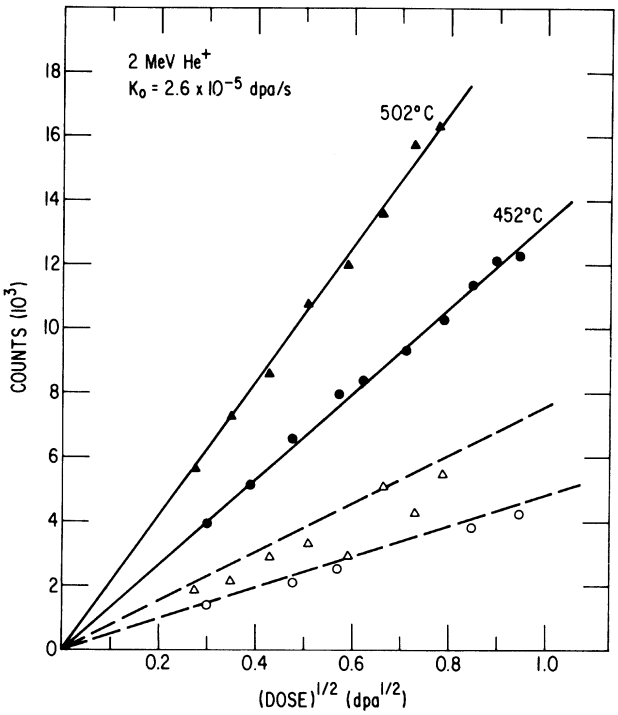

FIG. 4. Integral yields as a function of the square root of dose at 452 °C and 502 °C. The closed symbols indicate the Ni yields and the open symbols the Si yields. The solid lines are drawn through the Ni yields. The dashed lines for the Si yields were calculated relative to the Ni yields.

(from 12.7 to 23.5 at. %). To minimize possible systematic errors of this type, the yields for Ni and Si were averaged to obtain the γ' thickness. In a few cases, however, the scatter in the Si yields was too large to obtain reliable results and then only the Ni yields were employed.

Since each yield in Fig. 4 represents the average composition during the collection period of a spectrum, each dose correspondingly represents an "effective" dose (or time) ϕ', which is the dose that would have been required to produce the yield measured in each difference spectrum. This effective dose was obtained by equating the function describing the yield from the γ' layer as a function of dose $f(\phi')$ to the average yield determined in each difference spectrum, i.e.,

$$f(\phi')=\frac{1}{\phi_2-\phi_1}\int_{\phi_1}^{\phi_2} f(\phi)d\phi \ . \tag{1a}$$

If it is assumed that $f(\phi)$ obeys a simple power law,

$$f(\phi)=A\phi^n \ , \tag{1b}$$

then the effective dose is

$$\phi'=\left[\frac{1}{n+1}\frac{\phi_2^{n+1}-\phi_1^{n+1}}{\phi_2-\phi_1}\right]^{1/n} . \tag{1c}$$

For $(\phi_2-\phi_1)\ll\phi_1$, $\phi'=\phi_1$, i.e., the effective dose is independent of n. When $(\phi_2-\phi_1)\sim\phi_1$, however, ϕ' depends on n, but only weakly for reasonable values of n. For example, the second spectrum in each series was collected between 5 and 15 min. If $n=\frac{1}{2}$, as indicated by our results, (c.f. Figs. 5–7), $\phi'=9.78$ min (in units of time). If instead, the growth of the γ' layer were linear in time, i.e., $n=1$, then $\phi'=10$ min.

To convert integral yields to layer thicknesses a computer-simulation program for RBS was employed.[14] Values for the He stopping powers used in the program were obtained from the literature.[10] It was assumed in the simulation that the γ' layer had a uniform composition containing 23.5 at. % Si. The exact concentration of Si in the layer is not critical for the analysis of the segregation since the integrated yield in the difference spectra determines the net change in the Si concentration in the surface region, and it is this quantity which is of interest. If the usual procedure of using the difference in energy between the front and back edges of some layer in the RBS spectra had been employed to determine the layer thickness, then the exact solute concentration everywhere in the layer would have had to be known.

The thicknesses of the γ' layers for several of the He irradiations for which a dose rate of 3.1×10^{-4} dpa-s^{-1} was employed, are plotted as a function of the square root of dose in Fig. 5. Similar data are shown in Fig. 6 for the He irradiation at a lower dose rate, 2.6×10^{-5} dpa s^{-1}, and in

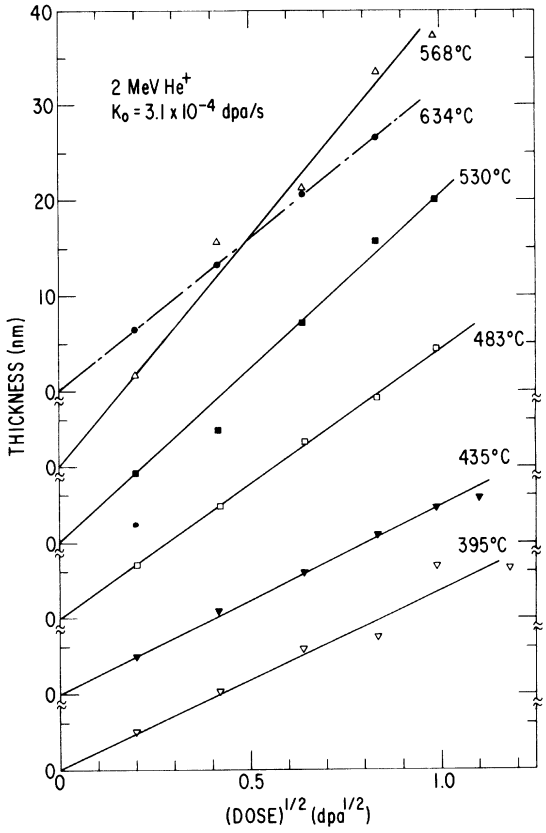

FIG. 5. Thickness of the γ' surface layer as a function of the square root of dose for 2.0-MeV He irradiation at various temperatures. The dose rate K_0 was 3.1×10^{-4} dpa per s.

Fig. 7 for a Li irradiation. In all cases the growth of the γ' layer follows a square root of dose dependence. For the He irradiations the square root of dose dependence was observed up to ~ 1 dpa; then the specimens blistered. For the Li irradiation the square root of dose dependence could be verified to ~ 5 dpa.

The slopes of the lines in Figs. 5–7 are growth-rate constants and contain information regarding the kinetics of RIS, i.e., the temperature and dose-rate dependences. The growth-rate constants for the He irradiations at both dose rates are plotted as a function of inverse temperature in an Arrhenius plot in Fig. 8. The growth rates during He irradiation can be fitted by a straight line for temperatures between ~ 400 °C and ~ 560 °C. The slope of this line yields an apparent activation enthalpy of 0.30 ± 0.04 eV for the layer growth. Also in this temperature range, the growth-rate constant decreases with increasing dose rate. At temperatures above 560°, a significant decrease in the segregation rate with temperature is evident. The data for $T > 600$ °C can be fitted by a line which yields an apparent activation enthalpy of -0.75 ± 0.15 eV. It is also observed in the high-temperature regime that the growth-rate constant becomes independent of dose rate. There is one datum at 345 °C which falls well below the line drawn through the other data. We currently suspect that the suppression of segregation at this temperature is due to radiation-induced internal sinks. The useful temperature ranges for determining the slopes in the Arrhenius plot correspond to relative changes in $1/T$ of $\lesssim 1.2$. Since the range in $1/T$ is small, accurate segregation measurements were essential in order to obtain reasonably accurate activation enthalpies.

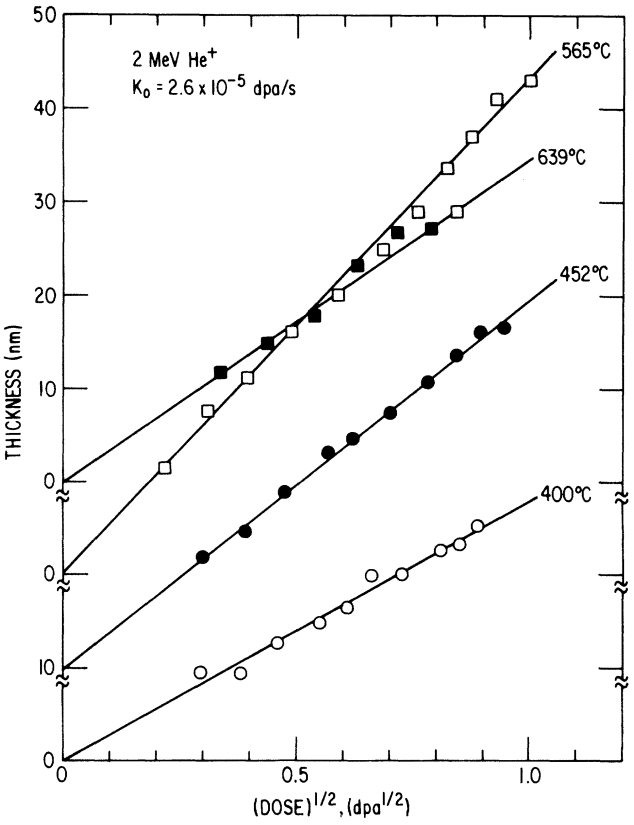

FIG. 6. Thickness of the γ' surface layer as a function of the square root of dose for 2.0-MeV He irradiation at various temperatures. The dose rate K_0 was 2.6×10^{-5} dpa per s.

IV. THEORETICAL MODEL

In this section we derive relations for the dose, dose-rate, alloy concentration, and temperature dependences of the growth of the γ' layer which develops at the irradiated surface of Ni-Si alloys. These relations have been previously derived by Okamoto *et al.*[15] In the derivation here we begin with the appropriate rate equations and explicitly show the approximations included in the model. Before writing down these rate equations we briefly describe the segregation model. A general review of the theory of RIS can be found elsewhere.[16]

Basically RIS requires two conditions, that there are persistent point-defect fluxes in the alloy, and that there is a preferential coupling of solute to these fluxes. The fluxes can arise from spatial nonhomogeneities in either the defect production or the defect annihilation. For 2.0-MeV He irradiation the defect-production distribution is nearly homogeneous within the first micrometer of the surface. The surface, however, is a spatially nonuniform sink. Solute can preferentially couple to the defect fluxes by two mechanisms, the inverse Kirkendall effect and the formation of mobile defect-solute complexes. The inverse Kirkendall effect causes segregation by either a preferential jumping of one species into vacancies, or a preferential migration of mobile interstitials via one species. For example, if there is a vacancy flux to a sink, then the species which preferentially jumps into the vacancies will establish a solute flux away from the sink. The other coupling mechanism involves the formation of mobile point-defect-solute complexes. The binding of solute to either

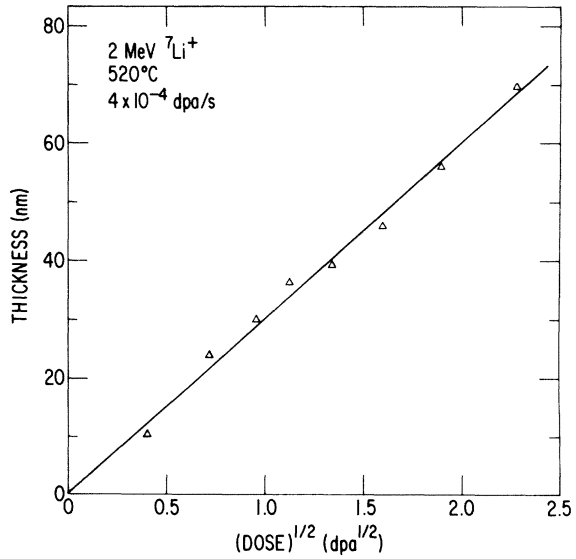

FIG. 7. Thickness of the γ' surface layer as a function of the square root of dose for 2.0-MeV Li irradiation at 520 °C. The dose rate K_0 was 4×10^{-4} dpa per s.

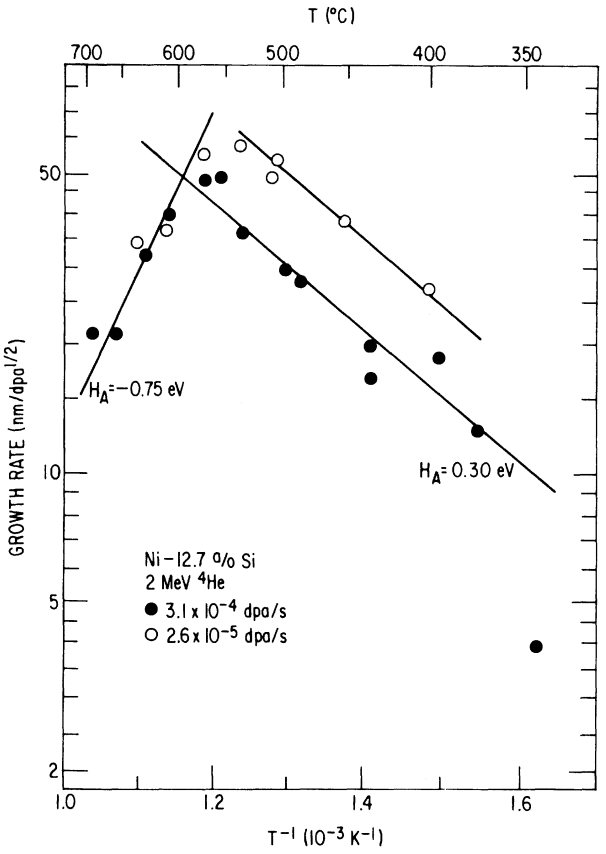

FIG. 8. Arrhenius plot of the growth-rate constant for two dose rates 3.1×10^{-4} dpa per s (closed symbols) and 2.6×10^{-5} dpa per s (open symbols).

vacancies or self-interstitial atoms (SIA's) induces the solute to be transported along with the defects to sinks. It is not possible to determine which coupling mechanism predominates by considering only the direction of the segregation, and in fact the coupling mechanism has not been clearly established in any system. For Ni-Si, however, there is evidence that suggests that the formation of mobile SIA-solute complexes is the dominant mechanism. This evidence includes the observation that Si is an efficient trap for SIA's in Ni,[17,18] indications that a Si-SIA complex is mobile below room temperature,[17,19] and theoretical estimates of high-binding energies in metals between SIA's and undersized solute atoms such as Si in Ni.[20] We thus assume that the formation and migration of Si-SIA complexes is the dominant coupling mode in Ni-Si alloys.

The chemical rate equations near the surface for SIA's, vacancies, Si-SIA complexes, and free solute are

$$\frac{\partial C_i}{\partial t}=K_0-K_{iv}C_iC_v-K_{i\mathrm{Si}}C_iC_{\mathrm{Si}}^f+K_dC_c+D_i\frac{\partial^2}{\partial x^2}C_i\ , \tag{2a}$$

$$\frac{\partial C_v}{\partial t}=K_0-K_{iv}C_iC_v-K_{vc}C_vC_c+D_v\frac{\partial^2}{\partial x^2}C_v\ , \tag{2b}$$

$$\frac{\partial C_c}{\partial t}=K_{i\mathrm{Si}}C_iC_{\mathrm{Si}}^f-K_{vc}C_vC_c-K_dC_c+D_c\frac{\partial^2}{\partial x^2}C_c\ , \tag{2c}$$

$$\frac{\partial C_{\mathrm{Si}}^f}{\partial t}=-K_{i\mathrm{Si}}C_iC_{\mathrm{Si}}^f+K_{vc}C_vC_c+K_dC_c+D_{\mathrm{Si}}\frac{\partial^2}{\partial x^2}C_{\mathrm{Si}}^f\ , \tag{2d}$$

where K_0 is the production rate, $K_{vc}=(4\pi r/\Omega)(D_v+D_c)$, $K_{iv}=(4\pi r/\Omega)(D_i+D_v)$, K_d is the dissociation rate of complexes, and $K_{i\mathrm{Si}}=(4\pi r/\Omega)D_i$. The quantities C_i, C_v, C_c, and C_{Si}^f refer to the self-interstitial, vacancy, SIA-Si complex, and free Si concentration, respectively. The parameter r is the effective interaction radius[21] for the relevant reaction; here for convenience all the radii are assumed equal. Ω is the atomic volume. The diffusion coefficients D_v, D_i, and D_c are for vacancies, SIA's, and complexes, respectively, and all have the form

$$D=D_0e^{-H_m/kT}\ , \tag{3}$$

where H_m is the migration enthalpy of the defect. These time-dependent equations cannot be solved analytically. We assume, however, that there is a moving coordinate systems x^* in which the different specie concentrations are in steady state and that this coordinate system is related to the stationary laboratory coordinate system by some function of time, i.e.,

$$\frac{\partial C(x^*)}{\partial t}=0\ \text{ where } x=x^*f(t)\ . \tag{4}$$

This behavior is often observed for diffusion phenomena where there are semiinfinite boundary conditions.[22] Justification of this assumption is given below. We make the additional assumption that solute can diffuse only via complexes, i.e., $D_{\mathrm{Si}}=0$. Setting Eqs. 2(a)–2(d) to zero and adding Eqs. 2(c) and 2(d) yield

$$D_c\frac{\partial^2}{\partial x^{*2}}C_c=0\ , \tag{5}$$

for which the solution is

$$C_c(x^*)=ax^*+b\ . \tag{6}$$

Figure 9 illustrates the model. In the bulk, far from the surface sink, the concentration of complexes has a con-

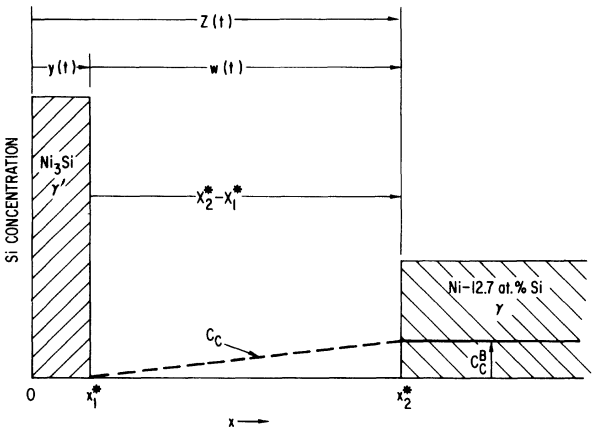

FIG. 9. Schematic representation of the segregation model. Self-interstitial atom-Si complexes form in the bulk (γ), diffuse down the complex-gradient across the diffusion layer, and contribute to the growth of the γ' layer.

stant value C_c^B. Its value is calculated below. At the surface there is a layer of γ'. We therefore use Eq. (6) between these two regions, i.e., in the diffusion layer, and apply the boundary conditions

$$C_c(x^*=x_1^*)=0$$

and

$$C_c(x^*=x_2^*)=C_c^B .$$

We thus assume that there are sharp interfaces at both sides of the diffusion layer. The flux J of complexes across the diffusion layer is obtained from the relations

$$J=D_c\frac{\partial C_c}{\partial x}=D_c\frac{\partial C_c}{\partial x^*}\frac{1}{f(t)} =D_c\frac{C_c^B}{(x_2^*-x_1^*)}\frac{1}{f(t)}=D_c\frac{C_c^B}{w(t)} , \tag{7}$$

since

$$w(t)=(x_2^*-x_1^*)f(t) .$$

As shown in Fig. 9

$$\frac{dw}{dt}=\frac{dz}{dt}-\frac{dy}{dt} . \tag{8}$$

Equation (8) can be related to Eq. (7) by using expressions for the conservation of solute

$$\frac{dy}{dt}=\frac{J}{C_{\rm Si}^{\gamma'}}$$

and

$$\frac{dz}{dt}=\frac{J}{C_{\rm Si}^{\gamma}} . \tag{9}$$

$C_{\rm Si}^{\gamma'}$ and $C_{\rm Si}^{\gamma}$ are the Si concentrations in the γ' and bulk alloy, respectively. By substituting $dt=d\phi/K_0$ in Eq. (8), and integrating we obtain

$$w(\phi)=[(2D_cC_c^B)(1/C^{\gamma}-1/C^{\gamma'})/K_0]^{1/2}\phi^{1/2} . \tag{10}$$

Using this expression with Eqs. (7) and (9) we arrive at the expression for the thickness of the γ' layer

$$y(\phi)=\left[\frac{2C_{\rm Si}^{\gamma}C_c^B}{C_{\rm Si}^{\gamma'}(C_{\rm Si}^{\gamma'}-C_{\rm Si}^{\gamma})}\frac{D_c}{K_0}\right]^{1/2}\phi^{1/2} . \tag{11}$$

We next solve for the bulk concentration of complexes, C_c^B. In the bulk the system is in true steady state, i.e., $\partial C_c^B/\partial t=0$, and no gradients exist, $(\partial C_c^B/\partial x)=0$. As the surface is not the dominant sink for defects in the bulk, we explicitly include a bulk concentration of sinks C_s. The appropriate rate equations are

$$\frac{\partial C_i}{\partial t}=K_0-K_{iv}C_iC_v-K_{i\rm Si}C_iC_{\rm Si}^f-K_{is}C_iC_s=0 , \tag{12a}$$

$$\frac{\partial C_v}{\partial t}=K_0-K_{iv}C_iC_v-K_{vc}C_vC_c^B-K_{vs}C_vC_s=0 , \tag{12b}$$

$$\frac{\partial C_c}{\partial t}=K_{i\rm Si}C_iC_{\rm Si}^f-K_{vc}C_vC_c^B-K_{cs}C_c^BC_s=0 , \tag{12c}$$

where

$$K_{vs}=\frac{4\pi r}{\Omega}D_v ,$$

$$K_{is}=\frac{4\pi r}{\Omega}D_i ,$$

and

$$K_{cs}=\frac{4\pi r}{\Omega}D_c .$$

At a temperature of ~ 500 °C and $K_0\sim 3\times 10^{-4}$ dpa s^{-1}, the vacancy and complex concentrations are small ($\lesssim 10^{-2}$ at. %) relative to the free-solute concentration $C_{\rm Si}^f$ ($\sim 10\%$). Thus the dominant reaction for self-interstitials is the formation of complexes.

$$K_{i\rm Si}C_iC_{\rm Si}^f=K_0 , \tag{13}$$

so that

$$K_0-K_{vc}C_vC_c^B-K_{vs}C_vC_s=0 , \tag{14a}$$

and

$$K_0-K_{vc}C_vC_c^B-K_{cs}C_c^BC_s=0 . \tag{14b}$$

The solutions to Eqs. (14) are

$$C_v=-\frac{K_{cs}C_s}{2K_{vc}}+\left[\frac{K_0K_{cs}}{K_{cv}K_{vs}}+\frac{K_{cs}^2C_s^2}{4K_{vc}^2}\right]^{1/2} , \tag{15a}$$

$$C_c^B=-\frac{K_{vs}C_s}{2K_{vc}}+\left[\frac{K_0K_{vs}}{K_{cv}K_{cs}}+\frac{K_{vs}^2C_s^2}{4K_{vc}^2}\right]^{1/2} . \tag{15b}$$

In the regime that defects are lost predominantly through recombination rather than to sinks, i.e.,

$$4K_0\gg K_{vs}K_{cs}C_s^2/K_{vc} ,$$

Eqs. (15) reduce to

$$C_v=\left[\frac{K_0K_{cs}}{K_{vc}K_{vs}}\right]^{1/2} \tag{16a}$$

and

$$C_c^B=\left[\frac{K_0K_{vs}}{K_{vc}K_{cs}}\right]^{1/2} . \tag{16b}$$

Substituting this value of C_c^B into Eq. (11) yields

$$y(\phi)=\left[\frac{2C_{\rm Si}^{\gamma}\left[\dfrac{K_0D_v}{(4\pi r/\Omega)(D_v+D_c)D_c}\right]^{1/2}D_c/K_0}{C_{\rm Si}^{\gamma'}(C_{\rm Si}^{\gamma'}-C_{\rm Si}^{\gamma})}\right]^{1/2}\phi^{1/2} . \tag{17}$$

The model, according to Eq. (17), makes the following predictions for the recombination limited regime.

(1) Dose dependence: $y(\phi)\propto\phi^{1/2}$.

(2) Dose-rate dependence (for a constant dose): $y(K_0)\propto K_0^{-1/4}$.

(3) Alloy concentration dependence:

$$y(C^{\gamma}) \propto \left[\frac{C^{\gamma}_{\mathrm{Si}}}{C^{\gamma'}_{\mathrm{Si}}(C^{\gamma'}_{\mathrm{Si}} - C^{\gamma}_{\mathrm{Si}})} \right]^{1/2} .$$

(4) Temperature dependence: For case (1) $D_c > D_v$,

$$y(T) \propto D_v^{1/4} \propto e^{-H_m^v/4kT} ,$$

and for case (2) $D_v > D_c$,

$$y(T) \propto D_c^{1/4} \propto e^{-H_m^c/4kT} .$$

At higher temperatures, the thermal equilibrium concentration of vacancies can no longer be neglected in the rate equations. In the limit that this contribution dominates the total vacancy concentration, the rate equation for complexes in the bulk becomes

$$K_0 - K_{vc} C_v C_c^B = 0 , \tag{16a'}$$

so that

$$C_c^B = \frac{K_0}{K_{vc} C_v} , \tag{16b'}$$

where

$$C_v \propto e^{-H_f^v/kT}$$

and H_f^v is the vacancy formation enthalpy. Substituting Eq. (16b') into Eq. (11) we obtain the same dependences on dose and solute concentration for high temperatures as for low temperature; however, the temperature and dose-rate dependences are different.

(1) Dose-rate dependence (for a constant dose):

$$y(K_0) \rightarrow \text{const} .$$

(2) Temperature dependence: For case (1) $D_c > D_v$

$$y(T) \rightarrow e^{H_f^v/2kT} ,$$

and for case (2) $D_v > D_c$

$$y(T) \rightarrow e^{H_f^v/2kT} e^{-(H_m^c - H_m^v)/2kT} .$$

One of the important assumptions in this model is that the boundary condition at the interface between the diffusion layer and bulk remains fixed in the x^* coordinate system, i.e., the quasi-steady-state condition. This assumption appears reasonable since the bulk can supply complexes at a constant rate which is determined by the dose rate and temperature. The flux of complexes leaving the bulk, however, decreases as the square root of dose. Therefore, the boundary condition should approach the limiting case of $C_c(x^* = x_2^*) = C_c^B$. Numerical solutions of the rate equations also support this assumption. They show that after a short transient period, the complex concentration increases nearly linearly with distance away from the γ-γ' interface and approaches the value of C_c^B before leveling off in the bulk region.[15]

V. DISCUSSION

The experiments described in Sec. II have established the following kinetic behavior for the growth of a γ' layer at the surface of an irradiated Ni—12.7 at. % Si alloy: (1) The thickness of the layer increases proportionately to the square root of dose throughout the temperature range from 370 °C to 700 °C. (2) The growth-rate constant [A in Eq. 1(b)] exhibits Arrhenius behavior at both high and low temperatures, but distinctly different values for the apparent activation enthalpy are found in the two temperature regimes. Above $\sim$590 °C the apparent activation enthalpy is -0.75 ± 0.15 eV, below $\sim$570 °C it is 0.30 ± 0.04 eV. (3) The growth-rate constant decreases as the dose rate increases in the low-temperature regime. Increasing the dose rate a factor of 10 reduces the layer thickness a factor of ~ 1.7. If it is assumed that $A \propto K_0^p$, the results yield $p \sim -0.22$. In the high-temperature regime the growth rate is independent of the dose rate.

In Sec. III a simple model for RIS in Ni-Si alloys was outlined. The model assumes that self-interstitial atoms form mobile, tightly bound complexes with Si atoms during irradiation and that the flux of these complexes to a sink at the γ-γ' interface underlies the growth of the γ' layer. Within this model, the experimental observations acquire a natural physical interpretation. The model illustrates that the observed apparent activation enthalpy for the growth-rate constant at low temperatures is equal to $\frac{1}{4}$ the enthalpy of migration of the slower moving defect, the vacancy or complex. Considering the evidence that the complex moves faster than the vacancy in Ni-Si,[17,18] and that the enthalpy of migration of the vacancy in pure Ni is 1.06 ± 0.06 eV,[23] we attribute the measured activation energy of 0.30 ± 0.04 eV to $\frac{1}{4}$ of the vacancy migration enthalpy in a Ni—12.7 at. % Si alloy. The close agreement between the vacancy migration enthalpies in pure Ni and in the alloy shows that Si solute does not significantly alter the vacancy mobility in Ni. A similar conclusion was drawn from diffuse x-ray scattering studies of electron irradiated Ni—1 at. % Si alloys.[17] At higher temperatures the model predicts that the growth-rate constant should have an apparent activation enthalpy equal to $-\frac{1}{2}$ the enthalpy of vacancy formation. The value obtained here, -0.75 ± 0.15 eV, is within the experimental uncertainty of being $-\frac{1}{2}$ of the vacancy formation enthalpy in pure Ni, 1.76 ± 0.05 eV.[24] By using the relation $H_b = H_f^v(\text{pure}) - H_f^v(\text{alloy})$ this set of values and uncertainties places an upper limit for the *effective* binding enthalpy of vacancies with Si of ~ 0.5 eV.

The observed temperature dependence is a consequence of the recombination of complexes and vacancies in the bulk. An increase in the vacancy concentration increases recombination and thereby reduces RIS. At low temperatures an increase in temperature lowers the vacancy concentration as radiation-induced vacancies migrate to sinks faster. This is the reason that the growth-rate constant at low temperatures reflects the vacancy migration enthalpy. At high temperatures, an increase in temperature increases the thermal equilibrium concentration of vacancies and hence reduces RIS. Thus the growth-rate constant at high temperatures reflects the enthalpy of vacancy formation.

An analogous argument can be made for the effect of dose rate on the growth-rate constant. At low temperatures an increase in dose rate increases the vacancy concentration so that the growth-rate constant is reduced. The model predicts that the growth-rate constant should depend on dose rate as $K_0^{-1/4}$, which is in agreement with the experiment. At high temperatures the thermal equilibrium concentration of vacancies is much greater than that due to irradiation so that changes in the dose rate do not significantly change the vacancy concentration nor, correspondingly, the growth-rate constant. The experimental verification of the derived relationship between the dose-rate and temperature dependences of the growth-rate constant constitutes a strong argument for the interpretation of the experiments. Moreover, these results provide confidence that kinetic measurements of RIS can be employed to investigate point-defect properties and defect interactions in alloys at high temperatures.

VI. CONCLUSIONS

In this paper we have described a method to perform quantitative measurements of the kinetics of radiation-induced segregation in alloys. The method involves the use of *in situ,* simultaneous, high-resolution RBS measurements of the flux of solute to a surface during light-ion irradiation. Application of the method to a Ni—12.7 at.% alloy revealed that (a) a layer of γ' grows at the surface of the irradiated alloy; (b) the layer grows proportionately to the square root of dose; (c) between 475 °C and 570 °C the growth-rate constant of the layer exhibits an apparent activation enthalpy of 0.03 ± 0.04 eV and depends on the $-\frac{1}{4}$th power of dose rate; (d) above 590 °C the growth-rate constant has an apparent activation enthalpy of 0.75 ± 0.15 eV and is independent of dose rate. A simple model of segregation was described in Sec. III which relates the observed kinetics of segregation to point-defect properties in Ni-Si alloys. It was found that the growth-rate constant at low temperatures is controlled by the enthalpy of vacancy migration, whereas at high temperatures it is controlled by the enthalpy of vacancy formation.

ACKNOWLEDGMENTS

The authors are grateful for the technical support of Mr. P. Baldo and Mr. L. J. Thompson. One of us (R.S.A.) wishes to acknowledge many helpful discussions with Dr. K. Schroeder and Dr. P. Ehrhart of the Kernforschungsanlage Jülich, Jülich, West Germany.

[1]P. R. Okamoto, S. D. Harkness, and J. J. Laidler, American Nuclear Society Transactions 16, 70 (1973); P. R. Okamoto and H. Wiedersich, J. Nucl. Mater. 53, 336 (1974).

[2]Workshop on Solute Segregation and Phase Stability During Irradiation, edited by J. O. Steigler [J. Nucl. Mater. 83 (1979)].

[3]*Phase Transformations During Irradiation,* edited by F. V. Nolfi, Jr. (Applied Sciences Publishers, London, 1983).

[4]*Phase Stability During Irradiation,* edited by J. R. Holland, D. I. Potter, and L. K. Mansur, (American Institute of Metallurgical Engineers, New York, 1981).

[5]D. I. Potter, L. E. Rehn, P. R. Okamoto, and H. Wiedersich, Scr. Metall. 11, 1095 (1977).

[6]L. E. Rehn, P. R. Okamoto, and H. Wiedersich, J. Nucl. Mater. 80, 172 (1979).

[7]D. I. Potter, P. R. Okamoto, H. Wiedersich, J. R. Wallace, and A. W. McCormick, Acta Metall. 27, 1175 (1979).

[8]R. S. Averback, L. E. Rehn, W. Wagner, P. R. Okamoto, and H. Wiedersich, Nucl. Instrum. Methods 194, 457 (1982).

[9]W. K. Chen, J. W. Mayer, and M.-A. Nicolet, *Backscattering Spectrometry* (Academic, New York, 1978).

[10]J. F. Ziegler, *Helium Stopping Powers and Ranges in All Elemental Matter* (Pergamon, New York, 1977).

[11]PINTO was written by R. Benedek. Details of the program appear in R. S. Averback, R. Benedek and K. L. Merkle, Phys. Rev. B 18, 4156 (1978).

[12]P. Lucasson, in *Fundamental Aspects of Radiation Damage in Metals,* edited by M. T. Robinson and F. W. Young, Jr. (U.S. Energy Research and Development Administration, Oak Ridge, Tenn., 1976), p. 42.

[13]W. Wagner, L. E. Rehn, and H. Wiedersich, Philos. Mag. A 45, 957 (1982).

[14]R. S. Averback, L. J. Thompson, M. Shalit, and J. Moyle, J. Appl. Phys. 53, 1342 (1982).

[15]P. R. Okamoto, L. E. Rehn, and R. S. Averback, J. Nucl. Mater. 108 & 109, 319 (1982).

[16]H. Wiedersich and N. Q. Lam, *Phase Transformations During Irradiation,* Ref. 3, p. 1.

[17]R. S. Averback and P. Ehrhart, J. Phys. F (to be published).

[18]P. R. Okamoto, L. E. Rehn, R. S. Averback, K.-H. Robrock, and H. Wiedersich, *Proceedings of Yamada Conference V on Point Defects and Defect Interactions in Metals,* edited by Jin-Ichi Takamura, Masao Doyama, and Michio Kiritani (University of Tokyo Press, Kyoto, Japan, 1982), p. 946.

[19]P. Moser, J. Verdone, W. Chambron, V. Hivert, and R. Pichon *Fifth International Conference on International Friction and Ultrasonic Attenuation in Crystalline Solids,* edited by D. Levy and K. Lücke (Springer, Berlin, 1975), Vol. 1, p. 239.

[20]P. H. Dederich, C. Lehmann, H. R. Schober, A. Scholz, and R. Zeller, J. Nucl. Mater. 69 & 70, 176 (1978).

[21]R. Sizmann, J. Nucl. Mater. 69-70, 386 (1978).

[22]See, e.g., Paul G. Shewnon, *Diffusion in Solids* (McGraw-Hill, New York, 1963), p. 13.

[23]S. K. Khanna and K. Sonnenberg, Radiat. Eff. 59, 91 (1981).

[24]L. C. Smedskjaer, M. J. Fluss, D. G. Legnini, M. K. Chason, and R. W. Siegel, J. Phys. F 11, 2221 (1981).